Check for updates

Geophysical Research Letters

RESEARCH LETTER
10.1029/2023GL106212

A Global Assessment of Heatwaves Since 1850 in Different Observational and Model Data Sets

Laura Lipfert[1], Ralf Hand[1], and Stefan Brönnimann[1]

[1]Institute of Geography and Oeschger Centre for Climate Change Research, University of Bern, Bern, Switzerland

Key Points:

- Using a forced AGCM ensemble can largely reproduce heatwave variability of the past 160 years throughout the Northern Hemisphere and Australia
- Sea surface temperature anomalies over the Central Pacific and Subpolar North Atlantic are connected to strong heatwave summers in North America and Europe
- During the El Nino 1877/1878 there was a global increase in heatwave days, while heatwaves in North America and parts of Europe decreased

Supporting Information:

Supporting Information may be found in the online version of this article.

Correspondence to:

L. Lipfert,
laura.lipfert@unibe.ch

Citation:

Lipfert, L., Hand, R., & Brönnimann, S. (2024). A global assessment of heatwaves since 1850 in different observational and model data sets. *Geophysical Research Letters*, *51*, e2023GL106212. https://doi.org/10.1029/2023GL106212

Received 1 SEP 2023
Accepted 21 DEC 2023

© 2024 The Authors.
This is an open access article under the terms of the Creative Commons Attribution-NonCommercial License, which permits use, distribution and reproduction in any medium, provided the original work is properly cited and is not used for commercial purposes.

Abstract We show that ModE-Sim, a global ensemble of atmospheric model simulations that uses observed ocean boundary conditions and radiative forcings providing 36 members with daily climate information can be used to in-depth analyze the known spatial and temporal variability of heatwaves in the Northern Hemisphere and Australia during the past 160 years. It can also be used to study actual past extreme events like heatwaves during the El Nino 1877/1878. To analyze past heatwaves we use a novel approach of a transient baseline climatology and compare to different observational data sets. Furthermore, we analyze sea surface temperature anomalies during the most extreme heatwave summers in North America, Europe and Australia and identify the most prominent anomaly patterns over the Subpolar North Atlantic and in the Central Pacific. Using a large ensemble of forced simulations, like ModE-Sim can consequently contribute to a better understanding of preindustrial heatwaves, their decadal variability and their driving mechanisms.

Plain Language Summary In this study we use an atmospheric model to look at historical heatwaves during the past 160 years. In several regions of the Northern Hemisphere and in Australia we can successfully reproduce heatwave variability that we see in observations with our model. One of the main reasons that we reproduce the evolution and distribution of past heatwaves with our model is that our simulations use observed Sea Surface Temperatures. We show that deviations from the mean Sea Surface Temperatures over the Central Pacific and the Subpolar North Atlantic are connected to more summer heatwaves over Europe and North America. We also look at the big El Nino event in 1877/1878 and show that there was global increase in heatwaves during this event, even though heatwaves in parts of Europe and in North America got less frequent. Overall, we show that this model is very useful to better understand extreme events like heatwaves during the preindustrial era where we only have very little or no climate observations.

1. Introduction

Changes in the occurrence and the characteristics of heatwaves since the middle of the 20th century are extensively studied in observational data sets (Perkins-Kirkpatrick & Lewis, 2020; Perkins et al., 2012; Zampieri et al., 2016) and model simulations (Hirsch et al., 2021; Perkins-Kirkpatrick & Gibson, 2017). There is a significant trend for several heatwave characteristics (frequency, days, intensity, duration) since the 1950s throughout the Northern and Southern Hemisphere (Perkins-Kirkpatrick & Lewis, 2020).

While there are multiple studies analyzing heatwaves in the late 20th century or in historical model simulations and projections, there are few studies analyzing heatwaves in the first half of the 20th or even the 19th century based on climate observations (station data or reanalysis products). In the early 20th century and during the preindustrial period good quality observational products are largely unavailable and studies are very regional or only analyze trends to compare to 21st century heatwaves using a fixed baseline climatology (Chapman et al., 2019; Della-Marta et al., 2007; Zampieri et al., 2016). Furthermore, analyzing heatwave characteristics in the CMIP5 and CMIP6 ensembles in comparison with observational data (Berkeley Earth) reveals that there are large biases between the observations and the model ensembles, likely due to an overestimation of the warming trend by the model simulations (Hirsch et al., 2021).

Sea surface temperature (SST) variability has been found to play a significant role in the occurrence of heatwaves. Phenomena like the El Nino Southern Oscillation (ENSO), the Indian Ocean Dipole or the Atlantic Multidecadal Oscillation can drive heatwaves by altering the circulation patterns and temperature gradients in the atmosphere, leading to a change in the variability of heatwaves in multiple regions (Domeisen et al., 2022; Reddy et al., 2021; Ruprich-Robert et al., 2018; Zhou & Wu, 2016). Tropical SST anomaly patterns such as ENSO are well known as drivers for heatwaves in adjacent regions as well as in several regions around the globe like Australia, North

19448007, 2024, 3, Downloaded from https://agupubs.onlinelibrary.wiley.com/doi/10.1029/2023GL106212 by Universitat Bern, Wiley Online Library on [19/02/2024]. See the Terms and Conditions (https://onlinelibrary.wiley.com/terms-and-conditions) on Wiley Online Library for rules of use; OA articles are governed by the applicable Creative Commons License

America or Europe (Loughran et al., 2019; Luo & Lau, 2020; Martija-Díez et al., 2021; Reddy et al., 2021). In contrast, extra-tropical Atlantic and Pacific SST anomaly patterns show strong non-stationarity. Consequently, it is difficult to find one dominant extra-tropical SST driver for each region and they are still subject to high uncertainties (Wehrli et al., 2019). Nevertheless, to understand changes in the variability of historical extreme events, such as heatwaves, it is crucial to understand changes in different climate modes and their connection to heat extremes (Morak et al., 2011).

In this study we use ModE-Sim, a global ensemble of atmospheric model simulations that uses observed ocean boundary conditions and radiative forcings and thereby provides 36 members with daily climate information of the past 600 years (Hand, Samakinwa, et al., 2023). Using such forced atmospheric model ensembles potentially provides a great opportunity to analyze heatwaves during the preindustrial period where observations are scarce or not at all available. Consequently, the aim of this study is to explore whether the ModE-Sim ensemble can be used to in-depth study preindustrial heatwaves and thereby contribute to reducing the high uncertainties in heatwave variability in the preindustrial era.

We focus on the past 160 years since 1850 to compare the model simulations against available observational reanalysis products. Using a model ensemble with 36 members allows us to in-depth study the statistical properties of rare past heatwaves. We analyze whether the model ensemble can represent heatwaves spatial and temporal variability of the past 160 years globally and address regional differences in the representation of heatwaves compared to the reanalysis. As ModE-Sim provides climate information of the past 600 years the aim of this analysis is to also verify whether ModE-Sim could potentially be used to analyze heatwaves between 1420 and 1850, a period where even less observations are available.

Furthermore, we investigate how the SST forcings based on observations that are used in the model simulations influence heatwave distribution in the Northern Hemisphere and Australia and which SST patterns are influencing the most extreme heatwave years in North America, Europe and Australia.

2. Data Sets and Methods

2.1. Data Sets

As model simulations we use Modern Era Simulations (ModE-Sim), a 36-member ensemble of simulations with the atmospheric general circulation model ECHAM6 that covers the period from 1420 to 2009 (Hand, Samakinwa, et al., 2023). For this study we use the simulation sets for the period 1850 to 2009 to compare against observational data sets. As ocean boundary conditions the model uses different realizations of HADISST2 (Rayner et al., 2003) and, to extend the available forcing data, recombinations of them (Hand, Samakinwa, et al., 2023). For the radiative (and volcanic) forcings the standard PMIP4 (Jungclaus et al., 2017) input is used. The atmospheric model is used in its low resolution configuration with a horizontal resolution of approximately 1.8°. The land-surface conditions for ECHAM6 are provided by the integrated land-surface model JSBACH (Reick et al., 2021). In ModE-Sim the configuration with non-dynamic vegetation is used. To analyze heatwave characteristics we re-grid all other data sets to model resolution using nearest neighbor remapping.

To compare our model results we need reanalysis or observational products which globally provide daily temperature values that also cover the preindustrial period before 1900. Consequently, our main reference is the NOAA 20th Century Reanalysis Version 3 ensemble mean daily mean temperature (Slivinski et al., 2019). This data set provides a global reanalysis that assimilates surface pressure observations from 1836 until today and also uses HADISST2 as ocean boundary conditions.

As an additional observational reference we use the EUSTACE data set which provides daily mean temperature estimates for the period 1850–2009. The EUSTACE project offers global multidecadal ensembles of daily surface air temperature combining satellite observations and different land station records (Rayner et al., 2020). The EUSTACE data set has many missing values where station-records are scarce, especially in the early period. For our analysis of heatwaves we therefore select, for every gridcell, the summer seasons without any missing values and only calculate the heatwave characteristics for this subset of the EUSTACE data. To further validate our model simulations we also use ERA5 daily mean surface temperature from 1959 to 2009 from the ECMWF (Hersbach et al., 2020).

19448007, 2024, 3, Downloaded from https://agupubs.onlinelibrary.wiley.com/doi/10.1029/2023GL106212 by Universitat Bern, Wiley Online Library on [19/02/2024]. See the Terms and Conditions (https://onlinelibrary.wiley.com/terms-and-conditions) on Wiley Online Library for rules of use; OA articles are governed by the applicable Creative Commons License

2.2. Methods

Heatwaves are defined as an exceedance of the 90th percentile of a baseline climatology of daily mean temperature for at least three consecutive days (Russo et al., 2014). The 90th percentile is calculated from a five day window surrounding the calendar day that is investigated for each gridcell (Dunn et al., 2020). We assess heatwaves over the extended summer season which is May to September for the Northern Hemisphere and November to March for the Southern Hemisphere (Perkins-Kirkpatrick & Gibson, 2017). When calculating the regional means for the IPCC AR6 regions we exclude the tropical regions (10°S–10°N).

We use two different approaches to define the baseline climatology which is used to calculate the 90th percentile threshold. First, we use a fixed baseline climatology for the reference period 1961–1990 (Dunn et al., 2020). Second, to assess heatwaves over the past 160 years and to compare the variability among data sets without a strong influence of the global warming trend we use a 31-year transient baseline climatology. This means, that for each year and each calendar day the 90th percentile is calculated using the surrounding 31 years. We do this separately for each ensemble member of the model simulations as well as for the reanalysis data sets. Using a linear detrending method over the whole period 1850–2009 could potentially lead to false results as the linear trend could be highly influenced by a strong event at the beginning of the timeseries where the uncertainty in the 20CRv3 reanalysis is still relatively large (Zampieri et al., 2016). The transient baseline climatology allows in-depth comparison of the variability of different heatwave characteristics going further back in time.

To assess heatwaves we calculate the characteristics heatwave days, average duration and cumulative intensity for each gridcell and compute means for selected AR6 regions (Figure 1c). Cumulative intensity thereby refers to the sum of the anomalies for all heatwave days in one season. Furthermore we investigate the anomalies of summer mean temperature to compare against the heatwave properties. We use Spearman Rank correlations to compare the variability of the observational and reanalysis data with the model ensemble mean and classify the significance at the 5% significance level.

In addition we identify the dominant SST anomalies (from the 1866–1995 mean) for strong heatwave years by making composites of the seasons with the 10% most heatwave days in North America, Europe and Australia over all ensemble members of the model simulations. Vice versa we then also analyze composites of heatwave years with the SST anomaly patters we identified in the first part of the analysis to validate whether there is an increase of heatwave days over the regions we would expect.

3. Results

3.1. Global Overview

To get a first overview of heatwaves in the ModE-Sim ensemble and the observational data sets, we analyze heatwave days across the Northern and Southern hemisphere using two different approaches: a fixed baseline climatology (1961–1990) and a 31-year transient climatology. Except for the timeseries (Figure 1a and Figure S1a in Supporting Information S1) this analysis is based on the 31-year transient climatology.

For the Northern Hemisphere there is significant correlation with the ModE-Sim ensemble mean for both, the fixed and the transient baseline climatology for the 20CRv3 ensemble mean, EUSTACE and the ERA5 reanalysis (Figures 1a and 1b). Also the strong trend resulting in a doubling to tripling of heatwave days since 1980 in both hemispheres, that is also supported by previous research on heatwave characteristics (Perkins-Kirkpatrick & Lewis, 2020), is well represented in the ModE-Sim ensemble.

Using the transient baseline climatology the temporal evolution and spatial distribution of heatwaves over the Northern Hemisphere is well represented in the ModE-Sim ensemble compared to 20CRv3 (Figures 1b–1e). The strongest differences between the two data sets are over Northern Africa and South East Asia with up to four more heatwave days per season in 20CRv3 than in the ModE-Sim ensemble mean. The good representation of heatwaves in the Northern Hemisphere by the model ensemble is also supported by comparing the distributions of heatwave days and average duration of the ModE-Sim ensemble members and 20CRv3 (Figures 1f and 1g). Most members have a similar distribution than the 20CRv3 reanalysis.

Differences between the two data sets can also be seen in the early part of the timeseries for the Northern hemispheric mean using the fixed baseline climatology. It is important to note that also the uncertainty in the 20CRv3

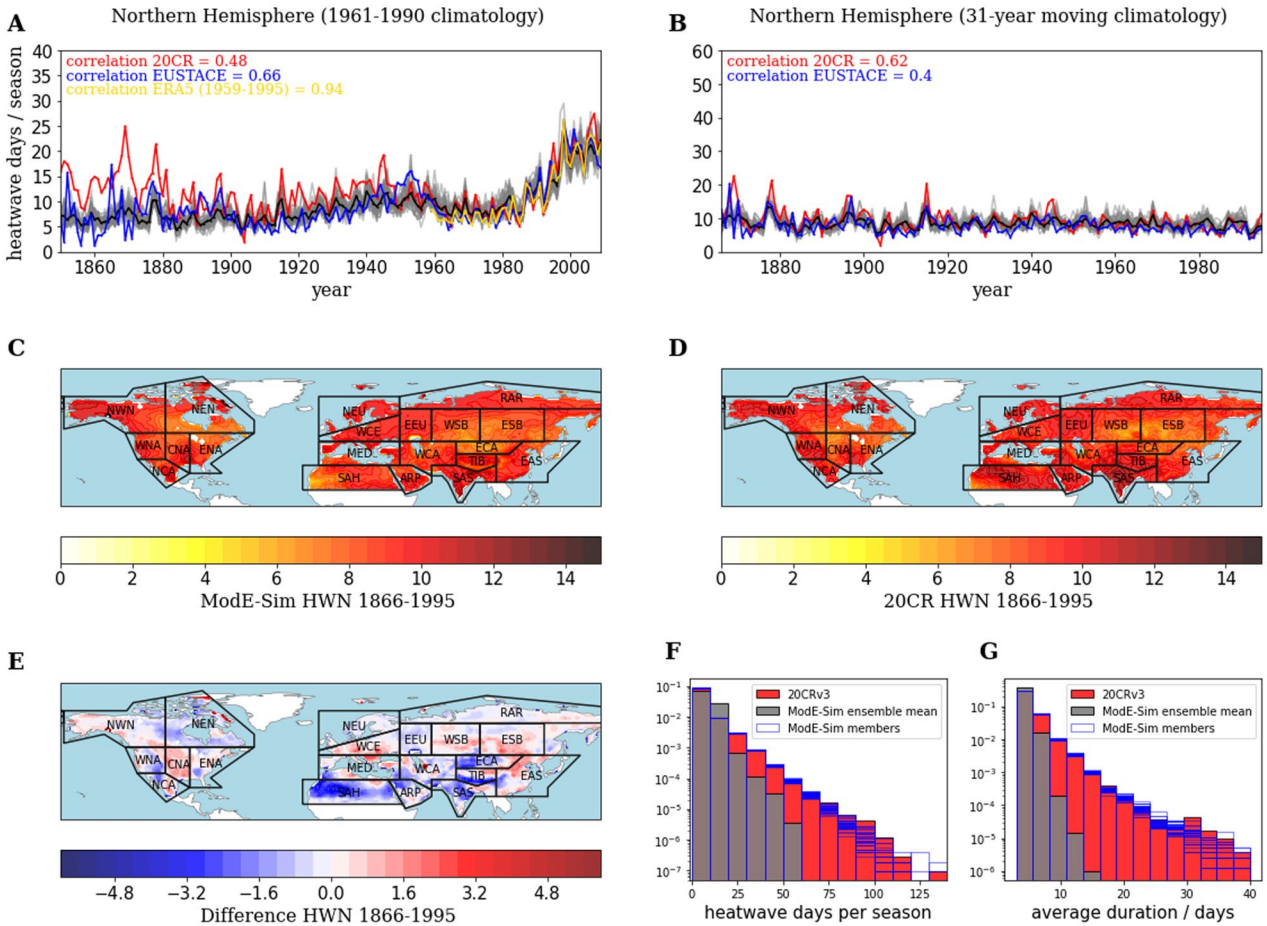

Figure 1. (a) Timeseries of Northern Hemisphere May-September heatwave days for 20CR (red), EUSTACE (blue), ERA5 (yellow) and ModE-Sim ensemble mean (black) and members (gray) with 1961–1990 baseline climatology. (b) Timeseries of Northern Hemisphere May-September heatwave days with 31-year transient baseline climatology. (c) 1866–1995 mean May-September heatwave days for ModE-Sim ensemble mean and (d) for 20CRv3. (e) Difference in 1866–1995 mean May-September heatwave days between ModESim and 20CRv3 (f) Distribution of heatwave days per season for all Northern Hemisphere gridcells for the ModE-Sim members (blue outlines), ModE-Sim ensemble mean (gray bars) and 20CRv3 (red bars). (g) Distribution of average heatwave duration. Subplots (c–g) are based on the 31-year transient baseline climatology.

reanalysis increases further back in time due to less and more uncertain observations (Slivinski et al., 2021), for instance in Northern Africa and South East Asia, which can explain this bias (Figure 1a). Furthermore, we analyzed for how many years heatwave days in the 20CRv3 reanalysis lie within the ensemble spread of ModE-Sim for each gridcell in the first and last 30 years of our analysis (Figure S2 in Supporting Information S1). Especially over Europe most years and gridcells lie within the ensemble spread for both time periods, while especially in the first 30-years (1866–1895) there are some discrepancies between 20CRv3 and the model ensemble over parts of North America, Northern Africa and South East Asia.

Correlations for the Southern hemispheric means are all significant but there are strong biases including areas with up to 20 more heatwave days per season in 20CR compared to the ModE-Sim ensemble mean (Figure S1 in Supporting Information S1). These biases could be related to the limited availability of observations in the Southern Hemisphere and therefore larger uncertainties in the reanalysis (Slivinski et al., 2021). Furthermore, analyzing the performance of ModE-Sim Hand, Samakinwa, et al. (2023) found a cold biases of the model ensemble in the Southern Hemisphere over India and South America, that agree with existing studies about ECHAM/MPI-ESM (Giorgetta et al., 2013). Consequently, the ability of ModE-Sim to analyze heatwaves in these Southern hemispheric regions, especially in the very early time period where observations are scarce is very limited. Due to these discrepancies, we focus the analysis in this study mainly on the Northern Hemisphere, but complement our research with the analysis of heatwave days over Australia, where despite some biases the

19448007, 2024, 3, Downloaded from https://agupubs.onlinelibrary.wiley.com/doi/10.1029/2023GL106212 by Universitat Bern, Wiley Online Library on [19/02/2024]. See the Terms and Conditions (https://onlinelibrary.wiley.com/terms-and-conditions) on Wiley Online Library for rules of use; OA articles are governed by the applicable Creative Commons License

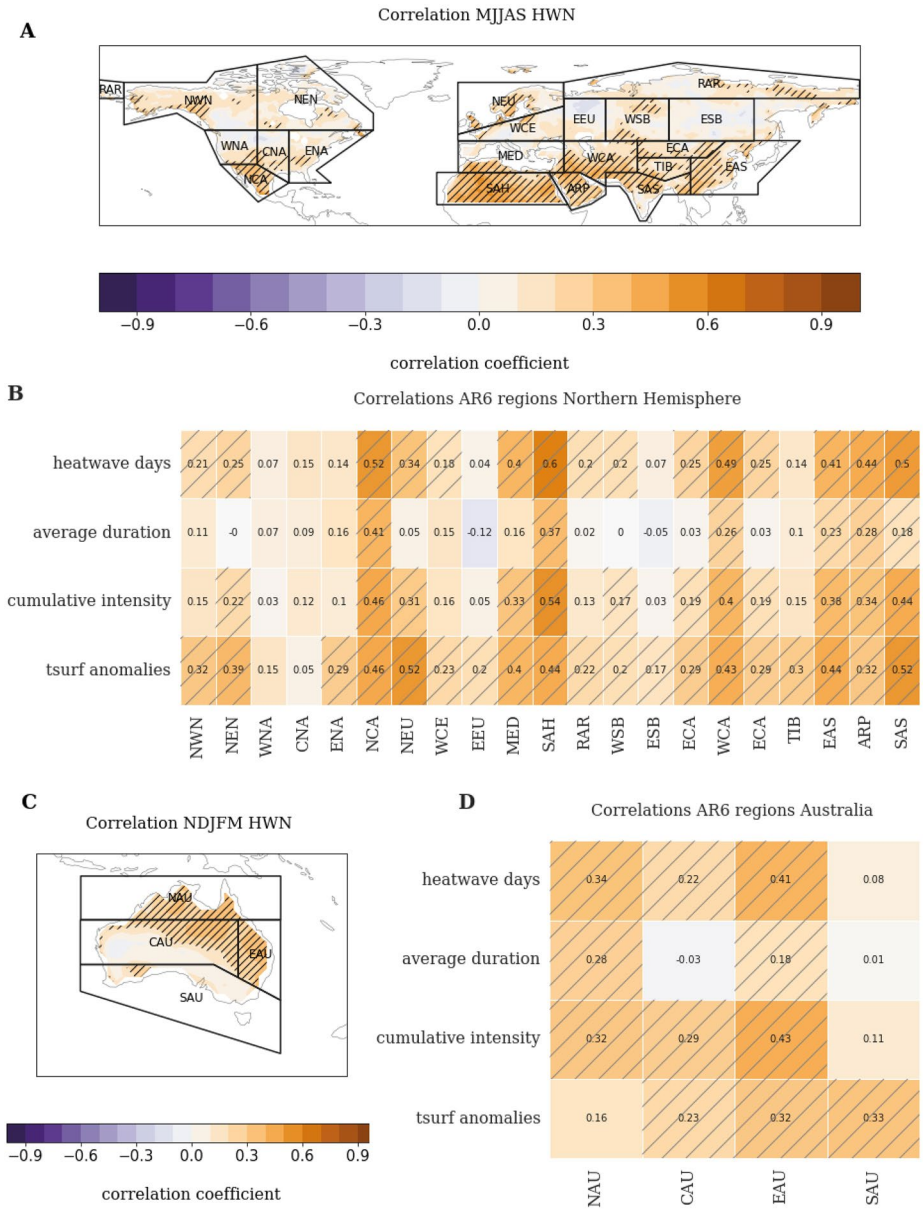

Figure 2. (a) Gridpoint based Spearman correlations of May-September heatwave days between ModE-Sim ensemble mean and 20CR. Hatching indicates significant correlation with a *p*-value below 0.05. (b) Correlations of May-September heatwave days, average duration, cumulative intensity and mean temperature anomalies between ModE-Sim and 20CR for AR6 regional means. (c) Gridpoint based Spearman correlations of November-March heatwave days between ModE-Sim ensemble mean and 20CR. (d) Correlation of November-March heatwave days, average duration, cumulative intensity and mean temperature anomalies between ModE-Sim and 20CR for AR6 regional means.

agreement between 20CR and ModE-Sim is better than for the rest of the Southern Hemisphere (Figure S3 in Supporting Information S1).

3.2. Regional Variability of Heatwaves Characteristics

Figure 2 shows that on the gridcell level and for the regional means we find areas with significant correlations between 20Crv3 and the ModE-Sim ensemble mean for all heatwave characteristics across the Northern Hemisphere and Australia. Correlations are mostly significant closer to the tropics (Southeast Asia, Central America, Northern Africa) but also partly over North America and Europe. We find that correlations are higher for the

19448007, 2024, 3, Downloaded from https://agupubs.onlinelibrary.wiley.com/doi/10.1029/2023GL106212 by Universitat Bern, Wiley Online Library on [19/02/2024]. See the Terms and Conditions (https://onlinelibrary.wiley.com/terms-and-conditions) on Wiley Online Library for rules of use; OA articles are governed by the applicable Creative Commons License

19448007, 2024, 3, Downloaded from https://agupubs.onlinelibrary.wiley.com/doi/10.1029/2023GL106212 by Universitat Bern, Wiley Online Library on [19/02/2024]. See the Terms and Conditions (https://onlinelibrary.wiley.com/terms-and-conditions) on Wiley Online Library for rules of use; OA articles are governed by the applicable Creative Commons License

regional means than if calculated for each gridpoint individually, due to less noise. However, for regions without any significant gridpoints (i.e., EEU, ESB), correlations for the regional mean heatwave characteristics are also not significant. In Central America, Sahara region, Western Central Asia and Northern and Eastern Australia correlations for heatwave days per season are even higher than for the yearly mean temperature anomalies. In the more Northern latitudes we find lower and mostly non-significant correlations between the model ensemble mean and 20CRv3. This suggests, that the influence of the forced signal in those regions is relatively small and that they are mainly dominated by internal variability. Perkins-Kirkpatrick and Lewis (2020) support this finding, arguing that especially in the higher latitudes the influence of internal variability on regional heatwave changes is considerably high.

Investigating the timeseries of heatwave days for some selected individual regions, we can conclude, that the ensemble spread of the model captures the variability that we see in the observational data sets for the regional means of Northern Europe, Central North America, Northern Central America and Eastern Australia (Figures 3a–3d).

Northern and Eastern Australia are the regions where we find the highest correlations for all three heatwave characteristics in Australia. In Eastern Australia our analysis reveals that there are only very few years with less than 10 heatwave days per season and that there are high inter-annual fluctuations in heatwave days compared to Northern Europe or North America (Figures 3a–3d). Previous research on heatwaves over Australia suggests that ENSO is the dominating climate mode with the highest influence on heatwave frequency over Northern and Eastern Australia due to a movement of the Walker circulation (Loughran et al., 2019). As the model ensemble is forced with observed SST, it is consistent that we find the highest correlations with observational reanalysis over this area. However, it should also be noted that despite the high correlations for Eastern Australia there is a significant bias between ModE-Sim and 20CRv3 heatwave days (Figure 3d and Figure S1e in Supporting Information S1).

To make our analysis globally complete correlations for the rest of the Southern Hemisphere are in Figure S4 in Supporting Information S1.

One advantage of a large ensemble of atmospheric simulations that uses observed external forcings is that we are able to see and investigate effects of past climatic events. As an example we analyzed the effect of the El Nino 1877/1878 on heatwave variability (Figures 3e–3h). This ENSO event caused a large disruption in global climate, starting late 1876 and peaked during boreal winter 1877/1878 (Figure S5 in Supporting Information S1). Previous studies suggest that this event caused the strongest surface temperature anomaly that was observed between 1850 and 2008 when removing the long-term trend, however there are high uncertainties in the observational data over this period (Aceituno et al., 2009; Kiladis & Diaz, 1986). Due to the high uncertainties in the observational data, we compare the 20CRv3 reanalysis with the daily data from ModE-Sim. During the peak phase of the event in boreal winter 1877/1878 we find strong positive anomalies in heatwave days throughout the Southern Hemisphere in both 20CRv3 and the ModE-Sim ensemble mean. The spatial distribution of heatwave days differs over Australia where ModE-Sim shows the strongest positive anomaly in the East (consistent with Loughran et al. (2019)) while 20CRv3 has the strongest positive heatwave days anomaly in the Southwest. Singh et al. (2018) find an increase in droughts over Eastern Australia in 1878 which could have co-occurred with positive temperature anomalies and heatwaves. Over the developing phase of the El Nino event in boreal summer 1877 there is an increase in heatwave days over the tropics in both data sets and a decrease in heatwave days over parts of Northern Europe and North America that is more pronounced in 20CRv3 than in the ModE-Sim ensemble mean.

3.3. Influence of SST Variations on Heatwaves

To further understand the relationships between heatwaves and SSTs and to validate, that the significant correlations in large parts of the Northern Hemisphere between the model ensemble and the observational data sets are related to the influence of the SST forcings on heatwaves we analyze SST composites for the 10% strongest heatwave years in North America and Europe in the ensemble of atmospheric model simulations (Figure 4).

For both regions the two most prominent SST anomalies in the composite analysis of the model ensemble are a negative anomaly in the Central Equatorial Pacific (together with a positive anomaly in the North Pacific) and a positive SST anomaly in the Sub-polar North Atlantic (Figures 4a and 4b). This suggests, that SST variations in these regions influence the most extreme heatwave years over North America and Europe. To further validate

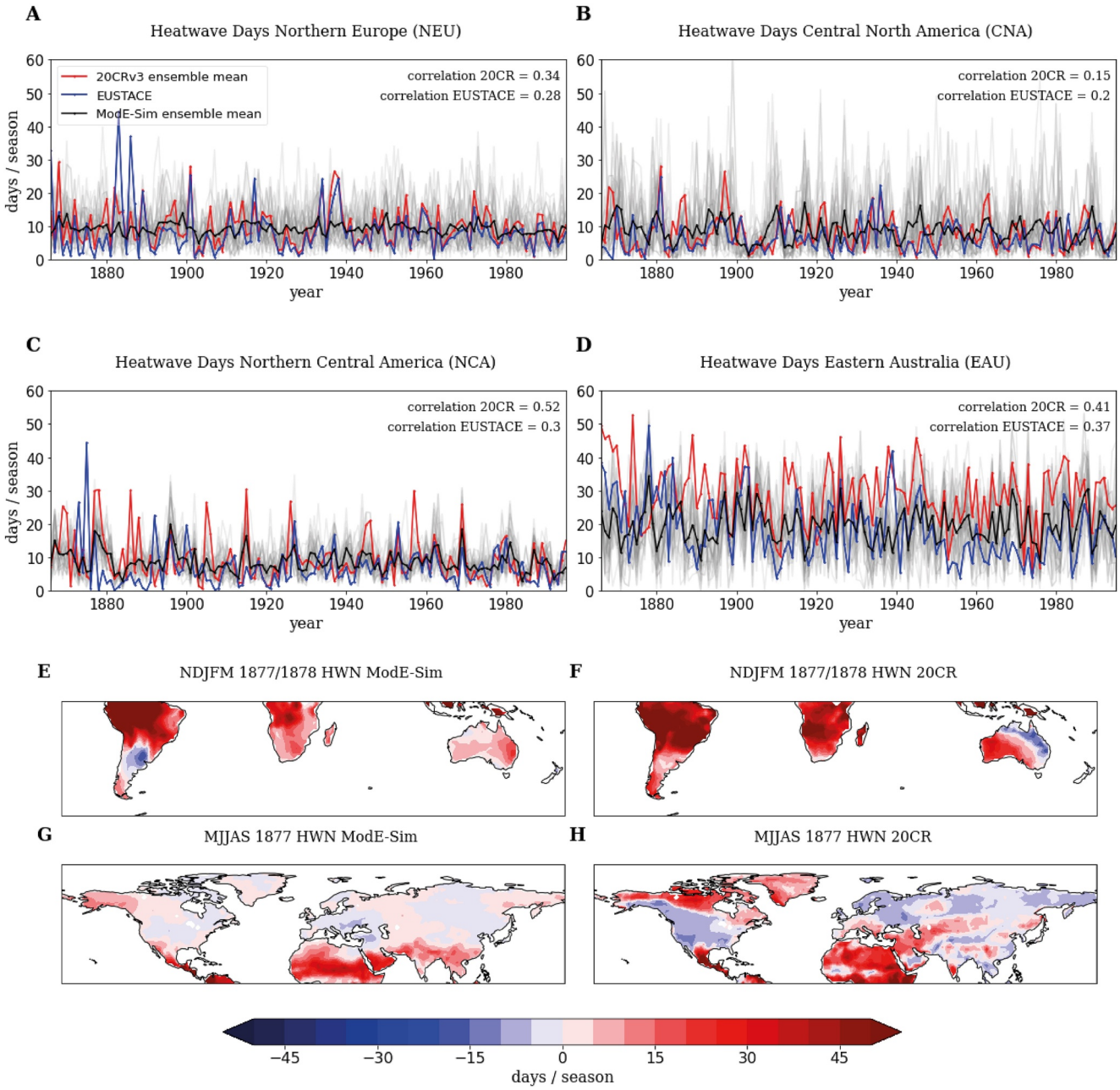

Figure 3. Timeseries of May-September heatwave days for 20CR (red), EUSTACE (blue), ModE-Sim ensemble mean (black) and ensemble members (gray) for (a) Northern Europe (b) Central North America (c) Northern Central America and (d) Eastern Australia. Correlations are Spearman Rank correlations. (e) 1877/1878 November-March heatwave days anomalies with respect to 1866–1995 for ModESim and (f) for 20CR. (g) 1878 May-September heatwave days anomalies with respect to 1866–1995 for ModESim and (h) for 20CR.

this we also look at heatwave days composites for all years in which the SST anomaly over the NINO3.4 region is below 0.5°C and for all years in which the SST anomaly over the Sub-polar North Atlantic is above 0.5°C (Figures 4c and 4d). For La Nina, the positive heatwave days anomalies are strongest over North America but also visible over parts of Europe as well as Central and East Asia. For the composites during a positive Sub-polar North Atlantic SST anomaly the effects on heatwave days are largest over Europe and the North Eastern Part of North America.

McKinnon et al. (2016) argue that the Pacific Extreme pattern with a positive SST anomaly over the Central North Pacific and a cold SST anomaly at the US West Coast is linked to extreme heat events in the Eastern

19448007, 2024, 3, Downloaded from https://agupubs.onlinelibrary.wiley.com/doi/10.1029/2023GL106212 by Universitat Bern, Wiley Online Library on [19/02/2024]. See the Terms and Conditions (https://onlinelibrary.wiley.com/terms-and-conditions) on Wiley Online Library for rules of use; OA articles are governed by the applicable Creative Commons License

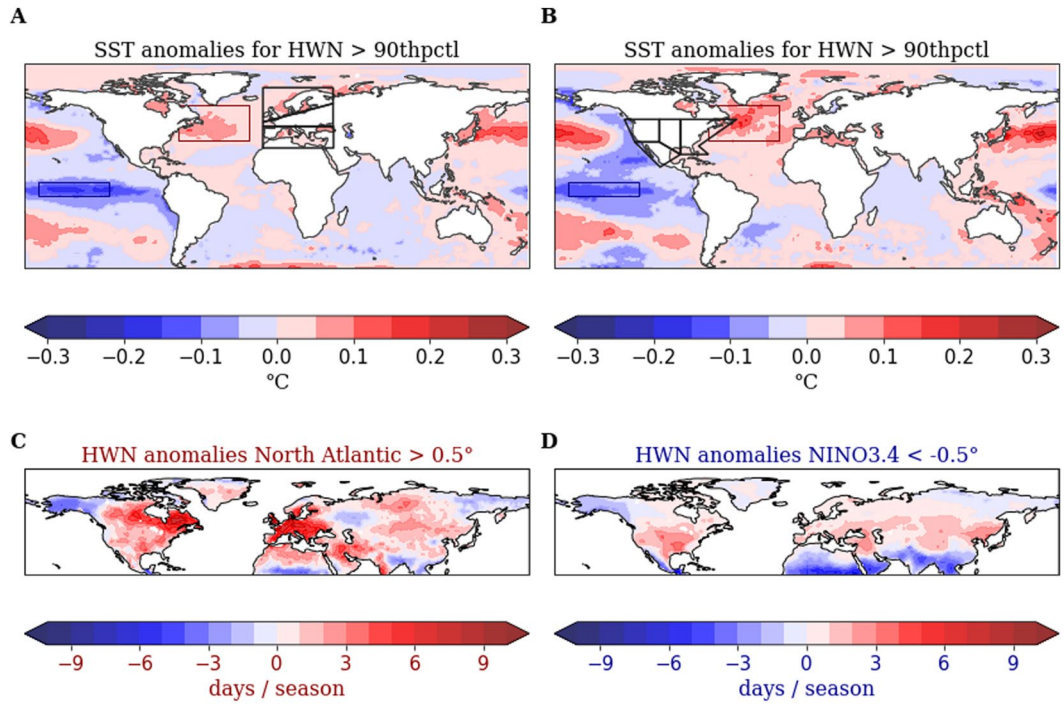

Figure 4. (a) Composite of ModE-Sim sea surface temperature (SST) anomalies where heatwave days over Europe are above the 90th percentile (1866–1995) (b) Composite of ModE-Sim SST anomalies where heatwave days over North America are above the 90th percentile (c) Composites of heatwave days anomalies for years where MJJAS North Atlantic SST anomaly (red box) is above 0.5°C and (d) where MJJAS NIN03.4 SST anomaly (blue box) is below −0.5°C.

US. In the ModE-Sim ensemble we also see this SST anomaly pattern in the composites analysis for extreme heatwave years over North America (Figure 4b). Furthermore, there are multiple studies linking La Nina (developing) summers to an increased heatwave occurrence over Western and Eastern Europe (Behera et al., 2013; Martija-Díez et al., 2021) as well as Northern America (Loikith & Broccoli, 2014; Luo & Lau, 2020). Using an ensemble of atmospheric simulations with observed SST forcings over the past 160 years, we can confirm this connection. Regarding the relationship between heatwave days and positive SST anomalies in the North Atlantic, Beobide-Arsuaga et al. (2023) found that positive spring SST in the Subpolar Gyre could be a precursor of European Summer Heatwaves. In our analysis we calculate the heatwave characteristics and the SST anomalies from May to September. A connection between early season SST anomalies and heatwaves could potentially explain why we see a connection between the strong heatwave years over Europe and positive SST anomalies in the Subpolar North Atlantic in the model ensemble investigating heatwaves since 1866.

In addition to the SST analysis of the Northern Hemisphere we also looked at composites for the 10% strongest heatwave years over Australia (Figure S6 in Supporting Information S1). As mentioned before, we find the main SST anomaly influencing heatwave days over Australia in the Central Pacific which suggests a connection to El Nino. Composites of all November to March Nino3.4 anomalies above 0.5°C also reveal that there is an increase in heatwave days across the whole Southern Hemisphere, especially in Southern Africa and Northern and Eastern Australia.

The composite analysis for the strongest heatwave years since 1866 further supports our suggestion that, the partly significant correlations in the Northern Hemisphere and Australia between the model ensemble and 20CR largely arise from the correct representation of the relationship between SSTs and heatwaves in ModE-Sim.

4. Conclusions and Discussion

With this analysis we show that a 36 member large ensemble of atmospheric model simulations that uses observed SST and radiative forcings well represents the spatial distribution and magnitude of heatwaves throughout the Northern Hemisphere (and Australia) (Figure 1). Many regions and gridpoints are significantly correlated with

19448007, 2024, 3, Downloaded from https://agupubs.onlinelibrary.wiley.com/doi/10.1029/2023GL106212 by Universitat Bern, Wiley Online Library on [19/02/2024]. See the Terms and Conditions (https://onlinelibrary.wiley.com/terms-and-conditions) on Wiley Online Library for rules of use; OA articles are governed by the applicable Creative Commons License

19448007, 2024, 3, Downloaded from https://agupubs.onlinelibrary.wiley.com/doi/10.1029/2023GL106212 by Universitat Bern, Wiley Online Library on [19/02/2024]. See the Terms and Conditions (https://onlinelibrary.wiley.com/terms-and-conditions) on Wiley Online Library for rules of use; OA articles are governed by the applicable Creative Commons License

the observational reanalysis which shows that the model ensemble can be used to analyze the decadal variability of heatwaves as well as individual past extreme heat events during the strong El Nino 1877/1878 (Figures 2 and 3). For the first time our analysis uses continuous daily reanalysis and model simulations during this event and can contribute to previous studies (Aceituno et al., 2009; Kiladis & Diaz, 1986) that there has been a global increase in heatwave days during the El Nino 1877/1878 event with most impacts in the Southern Hemisphere and decreasing heatwave days in North America and parts of Europe. Significant correlations between the model ensemble and the reanalysis likely arise due to the relationship between the observed SST forcings and heatwave variability. We find, that the most dominant SST anomalies during the 10% most extreme heatwave years over North America and Europe are a La Nina like negative anomaly over the Central Pacific and a positive anomaly over the Subpolar North Atlantic (Figure 4).

While we only investigated the SST forcings in the seasons parallel to the heatwaves it could also be beneficial to analyze SST patterns in the seasons prior to the heatwaves occurring (i.e., Beobide-Arsuaga et al., 2023). Furthermore, especially for the extra-tropical SST patterns it is hard to find one dominant pattern that is related to the most extreme events (Wehrli et al., 2019) and the mechanisms that can cause heatwaves that is, over Europe are very diverse (Domeisen et al., 2022). For example, the 2015 heatwave over Europe was linked to an extremely cold North Atlantic SST anomaly (Mecking et al., 2019) while we find a positive Subpolar SST anomaly related to extreme heatwave summers over Europe.

A further limitation of our analysis is the bias between the model simulations and the observation based data sets especially in the early period. The bias is especially large in the Southern Hemisphere (Figures S1 and S2 in Supporting Information S1) where uncertainties in the 20CRv3 reanalysis and the EUSTACE data set are also very pronounced due to limited observations (Rayner et al., 2020; Slivinski et al., 2021). Faranda et al. (2023) show that 20CRv3 can be used to analyze drought events over Western Europe caused by stationary heights suggesting that the reanalysis is suitable to analyze heatwaves over this area caused by similar processes which is consistent with our findings. Land-surface processes are also very important, especially for shorter duration heatwaves (Domeisen et al., 2022). While ModE-Sim uses the JSBACH land-surface as a boundary condition, 20CRv3 only assimilates pressure data. Consequently, uncertainties in short duration heatwaves caused by such processes are potentially larger in our analysis.

Compared to a study analyzing heatwaves in the CMIP5 + CMIP6 simulations (in comparison with the Berkeley Earth reanalysis) the ModE-Sim ensemble has lower biases for heatwave days and does not overestimate the 20th century warming trend (Hirsch et al., 2021). The lower biases in ModE-Sim are likely due to a combination of using observed forcings and a transient baseline climatology as detrending method that counteracts the warming trends. For a continuation of this analysis it would also be interesting to directly compare ModE-Sim to other atmospheric model ensembles.

We investigate the ModE-Sim ensemble since 1850, to compare to observation based data sets. By this, we verify that in several regions the model ensemble creates a plausible heatwave climatology and variance agreeing with observational data sets from different sources. However, the model simulations provide daily climate information from 1420 onward and can therefore in the future also be used to analyze preindustrial heatwaves of the past 600 years and their connections to SST and radiative forcings, especially with our novel approach using a transient baseline climatology. This analysis of heatwave variability and their connections to SST forcings in a novel large ensemble of forced atmospheric simulations consequently provides an important step toward a better understanding of preindustrial extreme events.

Data Availability Statement

The ModE-Sim simulations are available in Hand, Brönnimann, et al. (2023). The NOAA 20CRv3 reanalysis can be found via Slivinski et al. (2019). The daily mean temperature from the EUSTACE project was accessed via Brugnara et al. (2019) and the ERA 5 reanalysis can be obtained via Hersbach et al. (2020).

Acknowledgments
The work was supported by the European Research Council (ERC) under the European Unions Horizon 2020 research and innovation programme grant agreement No. 787574 (PALAEO-RA) and by the Swiss National Science Foundation (project WeaR 188701). The simulations where performed at the Swiss National Supercomputing Centre (CSCS).

References

Aceituno, P., Prieto, M. D. R., Solari, M. E., Martínez, A., Poveda, G., & Falvey, M. (2009). The 1877–1878 El Niño episode: Associated impacts in south America. *Climatic Change*, *92*(3–4), 389–416. https://doi.org/10.1007/s10584-008-9470-5

Behera, S., Ratnam, J. V., Masumoto, Y., & Yamagata, T. (2013). Origin of extreme summers in Europe: The indo-pacific connection. *Climate Dynamics*, *41*(3–4), 663–676. https://doi.org/10.1007/s00382-012-1524-8

Beobide-Arsuaga, G., Düsterhus, A., Müller, W. A., Barnes, E. A., & Baehr, J. (2023). Spring regional sea surface temperatures as a precursor of European summer heatwaves. *Geophysical Research Letters*, *50*(2), e2022GL100727. https://doi.org/10.1029/2022gl100727

Brugnara, Y., Good, E., Squintu, A. A., van der Schrier, G., & Brönnimann, S. (2019). The Eustace global land station daily air temperature dataset [Dataset]. Geoscience Data Journal, *6*(2), 189–204. https://doi.org/10.1002/gdj3.81

Chapman, S., Watkins, N. W., & Stainforth, D. A. (2019). Warming trends in summer heatwaves. *Geophysical Research Letters*, *46*(3), 1634–1640. https://doi.org/10.1029/2018gl081004

Della-Marta, P. M., Haylock, M. R., Luterbacher, J., & Wanner, H. (2007). Doubled length of western European summer heat waves since 1880. *Journal of Geophysical Research*, *112*(D15), D15103. https://doi.org/10.1029/2007jd008510

Domeisen, D. I., Eltahir, E. A., Fischer, E. M., Knutti, R., Perkins-Kirkpatrick, S. E., Schär, C., et al. (2022). Prediction and projection of heatwaves. *Nature Reviews Earth & Environment*, *4*, 1–15. https://doi.org/10.1038/s43017-022-00371-z

Dunn, R. J., Alexander, L. V., Donat, M. G., Zhang, X., Bador, M., Herold, N., et al. (2020). Development of an updated global land in situ-based data set of temperature and precipitation extremes: Hadex3. *Journal of Geophysical Research: Atmospheres*, *125*(16), e2019JD032263. https://doi.org/10.1029/2019jd032263

Faranda, D., Pascale, S., & Bulut, B. (2023). Persistent anticyclonic conditions and climate change exacerbated the exceptional 2022 European-mediterranean drought. *Environmental Research Letters*. https://doi.org/10.1088/1748-9326/acbc37

Giorgetta, M. A., Jungclaus, J., Reick, C. H., Legutke, S., Bader, J., Böttinger, M., et al. (2013). Climate and carbon cycle changes from 1850 to 2100 in mpi-esm simulations for the coupled model intercomparison project phase 5. *Journal of Advances in Modeling Earth Systems*, *5*(3), 572–597. https://doi.org/10.1002/jame.20038

Hand, R., Brönnimann, S., Samakinwa, E., & Lipfert, L. (2023). Mode-sim—A medium size AGCM ensemble to study climate variability during the past 600 years [Dataset]. World Data Center for Climate (WDCC) at DKRZ. Retrieved from https://www.wdc-climate.de/ui/entry?acronym=ModE-Sim

Hand, R., Samakinwa, E., Lipfert, L., & Brönnimann, S. (2023). Mode-sim—A medium-sized atmospheric general circulation model (AGCM) ensemble to study climate variability during the modern era (1420 to 2009). *Geoscientific Model Development*, *16*(16), 4853–4866. https://doi.org/10.5194/gmd-16-4853-2023

Hersbach, H., Bell, B., Berrisford, P., Hirahara, S., Horányi, A., Muñoz-Sabater, J., et al. (2020). The era5 global reanalysis [Dataset]. Quarterly Journal of the Royal Meteorological Society, *146*(730), 1999–2049. https://doi.org/10.1002/qj.3803

Hirsch, A. L., Ridder, N. N., Perkins-Kirkpatrick, S. E., & Ukkola, A. (2021). Cmip6 multimodel evaluation of present-day heatwave attributes. *Geophysical Research Letters*, *48*(22), e2021GL095161. https://doi.org/10.1029/2021gl095161

Jungclaus, J. H., Bard, E., Baroni, M., Braconnot, P., Cao, J., Chini, L. P., et al. (2017). The PMIP4 contribution to CMIP6—Part 3: The last millennium, scientific objective, and experimental design for the PMIP4 past1000 simulations. *Geoscientific Model Development*, *10*(11), 4005–4033. https://doi.org/10.5194/gmd-10-4005-2017

Kiladis, G. N., & Diaz, H. F. (1986). An analysis of the 1877–78 Enso episode and comparison with 1982–83. *Monthly Weather Review*, *114*(6), 1035–1047. https://doi.org/10.1175/1520-0493(1986)114<1035:aaotee>2.0.co;2

Loikith, P. C., & Broccoli, A. J. (2014). The influence of recurrent modes of climate variability on the occurrence of winter and summer extreme temperatures over North America. *Journal of Climate*, *27*(4), 1600–1618. https://doi.org/10.1175/jcli-d-13-00068.1

Loughran, T. F., Pitman, A. J., & Perkins-Kirkpatrick, S. E. (2019). The El Niño–southern oscillation's effect on summer heatwave development mechanisms in Australia. *Climate Dynamics*, *52*(9–10), 6279–6300. https://doi.org/10.1007/s00382-018-4511-x

Luo, M., & Lau, N.-C. (2020). Summer heat extremes in northern continents linked to developing ENSO events. *Environmental Research Letters*, *15*(7), 074042. https://doi.org/10.1088/1748-9326/ab7d07

Martija-Díez, M., Rodríguez-Fonseca, B., & López-Parages, J. (2021). ENSO influence on western European summer and fall temperatures. *Journal of Climate*, *34*(19), 8013–8031. https://doi.org/10.1175/jcli-d-20-0808.1

McKinnon, K. A., Rhines, A., Tingley, M., & Huybers, P. (2016). Long-lead predictions of eastern United States hot days from pacific sea surface temperatures. *Nature Geoscience*, *9*(5), 389–394. https://doi.org/10.1038/ngeo2687

Mecking, J., Drijfhout, S., Hirschi, J. J., & Blaker, A. (2019). Ocean and atmosphere influence on the 2015 European heatwave. *Environmental Research Letters*, *14*(11), 114035. https://doi.org/10.1088/1748-9326/ab4d33

Morak, S., Hegerl, G., & Kenyon, J. (2011). Detectable regional changes in the number of warm nights. *Geophysical Research Letters*, *38*(17), L17703. https://doi.org/10.1029/2011gl048531

Perkins, S. E., Alexander, L. V., & Nairn, J. (2012). Increasing frequency, intensity and duration of observed global heatwaves and warm spells. *Geophysical Research Letters*, *39*(20), 20714. https://doi.org/10.1029/2012gl053361

Perkins-Kirkpatrick, S. E., & Gibson, P. B. (2017). Changes in regional heatwave characteristics as a function of increasing global temperature. *Scientific Reports*, *7*(1), 1–12. https://doi.org/10.1038/s41598-017-12520-2

Perkins-Kirkpatrick, S. E., & Lewis, S. C. (2020). Increasing trends in regional heatwaves. *Nature Communications*, *11*(1), 1–8. https://doi.org/10.1038/s41467-020-16970-7

Rayner, N., Auchmann, R., Bessembinder, J., Brönnimann, S., Brugnara, Y., Capponi, F., et al. (2020). The Eustace project: Delivering global, daily information on surface air temperature. *Bulletin of the American Meteorological Society*, *101*(11), E1924–E1947. https://doi.org/10.1175/bams-d-19-0095.1

Rayner, N., Parker, D. E., Horton, E., Folland, C. K., Alexander, L. V., Rowell, D., et al. (2003). Global analyses of sea surface temperature, sea ice, and night marine air temperature since the late nineteenth century. *Journal of Geophysical Research*, *108*(D14), 4407. https://doi.org/10.1029/2002jd002670

Reddy, P. J., Perkins-Kirkpatrick, S. E., & Sharples, J. J. (2021). Interactive influence of ENSO and IOD on contiguous heatwaves in Australia. *Environmental Research Letters*, *17*(1), 014004. https://doi.org/10.1088/1748-9326/ac3e9a

Reick, C. H., Gayler, V., Goll, D., Hagemann, S., Heidkamp, M., Nabel, J. E., et al. (2021). Jsbach 3-the land component of the MPI earth system model: Documentation of version 3.2.

Ruprich-Robert, Y., Delworth, T., Msadek, R., Castruccio, F., Yeager, S., & Danabasoglu, G. (2018). Impacts of the Atlantic multidecadal variability on North American summer climate and heat waves. *Journal of Climate*, *31*(9), 3679–3700. https://doi.org/10.1175/jcli-d-17-0270.1

19448007, 2024, 3, Downloaded from https://agupubs.onlinelibrary.wiley.com/doi/10.1029/2023GL106212 by Universitat Bern, Wiley Online Library on [19/02/2024]. See the Terms and Conditions (https://onlinelibrary.wiley.com/terms-and-conditions) on Wiley Online Library for rules of use; OA articles are governed by the applicable Creative Commons License

Russo, S., Dosio, A., Graversen, R. G., Sillmann, J., Carrao, H., Dunbar, M. B., et al. (2014). Magnitude of extreme heat waves in present climate and their projection in a warming world. *Journal of Geophysical Research: Atmospheres*, *119*(22), 12–500. https://doi.org/10.1002/2014jd022098

Singh, D., Seager, R., Cook, B. I., Cane, M., Ting, M., Cook, E., & Davis, M. (2018). Climate and the global famine of 1876–78. *Journal of Climate*, *31*(23), 9445–9467. https://doi.org/10.1175/jcli-d-18-0159.1

Slivinski, L. C., Compo, G., Sardeshmukh, P., Whitaker, J., McColl, C., Allan, R., et al. (2021). An evaluation of the performance of the twentieth century reanalysis version 3. *Journal of Climate*, *34*(4), 1417–1438. https://doi.org/10.1175/jcli-d-20-0505.1

Slivinski, L. C., Compo, G. P., Whitaker, J. S., Sardeshmukh, P. D., Giese, B. S., McColl, C., et al. (2019). Towards a more reliable historical reanalysis: Improvements for version 3 of the twentieth century reanalysis system [Dataset]. Quarterly Journal of the Royal Meteorological Society, *145*(724), 2876–2908. https://doi.org/10.1002/qj.3598

Wehrli, K., Guillod, B. P., Hauser, M., Leclair, M., & Seneviratne, S. I. (2019). Identifying key driving processes of recent heatwaves and droughts (p. 21).

Zampieri, M., Russo, S., di Sabatino, S., Michetti, M., Scoccimarro, E., & Gualdi, S. (2016). Global assessment of heat wave magnitudes from 1901 to 2010 and implications for the river discharge of the Alps. *Science of the Total Environment*, *571*, 1330–1339. https://doi.org/10.1016/j.scitotenv.2016.07.008

Zhou, Y., & Wu, Z. (2016). Possible impacts of mega-El Niño/southern oscillation and Atlantic multidecadal oscillation on Eurasian heatwave frequency variability. *Quarterly Journal of the Royal Meteorological Society*, *142*(697), 1647–1661. https://doi.org/10.1002/qj.2759

19448007, 2024, 3, Downloaded from https://agupubs.onlinelibrary.wiley.com/doi/10.1029/2023GL106212 by Universitat Bern, Wiley Online Library on [19/02/2024]. See the Terms and Conditions (https://onlinelibrary.wiley.com/terms-and-conditions) on Wiley Online Library for rules of use; OA articles are governed by the applicable Creative Commons License